

DOI: 10.1070/QEL16146

A bolometer based on single-walled carbon nanotubes and hybrid materials

D.S. Kopylova, N.Yu. Boldyrev, V.Ya. Iakovlev, Yu.G. Gladush, A.G. Nasibulin

Abstract. **We have designed a bolometric IR detector based on freestanding aerosol synthesised carbon nanotubes and hybrid graphene materials deposited on a film suspended over a hole in the substrate. In this case, graphene serves as an absorber. The effect of the amount of the deposited absorber on the spectral characteristics, voltage sensitivity, response time and noise of the bolometer is investigated. The best response time is observed for the samples of pristine carbon nanotubes, whereas the hybrid sample with the largest amount of graphene demonstrates the highest sensitivity to radiation. Moreover, we have measured and analysed the bolometer parameters as functions of the ambient pressure and temperature, which has allowed us to determine the optimum operating conditions for the device.**

Keywords: *carbon nanotubes, bolometer, carbon nanomaterials, IR photodetectors.*

1. Introduction

Infrared (IR) detectors play an important role in modern technologies and are widely used in various fields, including the military applications. According to their operation principle, the two main types of IR detectors are photonic and thermal [1]. In photonic detectors, radiation is absorbed inside a material as a result of direct interaction of photons with charge carriers. These detectors include photovoltaic and photoemission detectors, photoconductive detectors, quantum well detectors, etc. In thermal detectors, incident radiation is absorbed by the material, which leads to a temperature rise and to a subsequent change in some physical properties of the material, such as resistance. Thermal detectors include pyroelectric detectors, thermocouples and bolometers [2, 3]. Unlike thermal detectors, photon detectors exhibit a wavelength-selective sensitivity, better signal-to-noise ratio and high response time. The advantages of thermal detectors are the simplicity of the design and the absence of necessity in cryogenic cooling, which greatly reduces energy consumption and cost of this type of devices, making them the most common for civil applications [2–4].

The search for new sensor materials for IR detectors is still urgent. Over the past ten years, carbon nanotubes have been used in the development of detectors based on different mechanisms of conductivity variation due to electromagnetic radiation [5]. The mechanism of the first type, photonic one, is related to the direct interaction of incident radiation with charge carriers – electrons and holes. The mechanism of the second type includes all thermal effects which result in heating the nanotubes by radiation and in changing their conductivity (metallic or semiconductor). Detectors based on the mechanism of the first type are represented by different photoconductors [6–9], Schottky diodes [10] and p–n junction detectors [11]. In these devices, a photon excites an exciton in carbon nanotubes (CNTs), which then decays into an electron and a hole between the valence and conduction bands. Then, carriers become separated by external or internal electric fields, and, as a consequence, a photocurrent or photovoltage arises.

In individual nanotubes, the photovoltaic effect is predominant [12–14] since in this case heat dissipates quickly due to high thermal conductivity of the tubes, which is not limited to the heat propagation through the tubes. In macroscopic structures (films) of nanotubes, on the contrary, the contribution of the direct photocurrent generation mechanism may be negligible because of very rapid relaxation of excitons. In this case, the absorbed energy is effectively transferred to the lattice vibrations through the electron–phonon interaction, which leads to a temperature rise and, as a result, causes the bolometric effect [13]. The possibility of designing a bolometer on carbon nanotubes was demonstrated by the group of Haddon and Itkis in 2006 [14, 15]. The authors showed that the electrical response of a CNT film to IR radiation is bolometric in nature, and also that the use of a suspended film leads to at least a fivefold increase in the device sensitivity compared to the case of a film lying on the substrate. Further studies of the CNT bolometer development have been conducted mainly in two directions. The first direction represents the use of thin suspended films of pristine nanotubes [16, 17], while the second assumes the development

D.S. Kopylova Skolkovo Institute of Science and Technology, ul. Nobelya 3, 143026 Moscow, Russia;e-mail: d.kopylova@skoltech.ru;
N.Yu. Boldyrev Institute of Spectroscopy, Russian Academy of Sciences, ul. Fizicheskaya 5, Troitsk, 142190 Moscow, Russia;
V.Ya. Iakovlev Skolkovo Institute of Science and Technology, ul. Nobelya 3, 143026 Moscow, Russia; Department of Applied Physics, Aalto University School of Science, P.O. Box 15100, FI-00076, Espoo, Finland;
Yu.G. Gladush Skolkovo Institute of Science and Technology, ul. Nobelya 3, 143026 Moscow, Russia; Institute of Spectroscopy, Russian Academy of Sciences, ul. Fizicheskaya 5, Troitsk, 142190 Moscow, Russia;
A.G. Nasibulin Skolkovo Institute of Science and Technology, ul. Nobelya 3, 143026 Moscow, Russia; Peter the Great St. Petersburg Polytechnic University, ul. Polyteknicheskaya 29, 195251 St. Petersburg, Russia; Department of Applied Physics, Aalto University School of Science, P.O. Box 15100, FI-00076, Espoo, Finland; e-mail: a.nasibulin@skoltech.ru

Received 27 May 2016; revision received 6 October 2016
Kvantovaya Elektronika **46** (12) 1163–1169 (2016)
Translated by M.A. Monastyrskiy

of a bolometric sensor based on a composite of various polymers and nanotubes [18–21].

Carbon nanotubes have a number of properties that allow one to consider them as a promising bolometric sensor. They have a low thermal capacity, high thermal conductivity and high strength. Moreover, the use of various chemical and physical methods for nanotube modification makes it possible to vary their optical and electrical properties over a wide range. According to Rogalski [2], the voltage sensitivity of a bolometric element (a ratio of the bolometer voltage response to the incident radiation power) is determined by the expression:

$$R_v = IR\alpha R_{th}\varepsilon, \quad (1)$$

where $R_{th} = G_{th}^{-1}$ is the thermal resistance; G_{th} is the thermal conductivity between a sensor and a substrate; ε is the coefficient of IR radiation absorption; $\alpha = R^{-1}dR/dT$ is the temperature coefficient of resistance; R is the sensor resistance; and I is the current through the sensor. Thus, the larger the coefficients α and ε and the lower the thermal conductivity, the higher the detector sensitivity. On the other hand, the bolometer operating speed is determined by a characteristic response time of the sensor to the change in irradiance:

$$\tau = C/G_{th}, \quad (2)$$

where C is the heat capacity of an absorber and a sensor. Consequently, the lower the sensor's heat capacity, the faster it reacts to changes in the intensity of IR radiation.

In the present study we have investigated bolometric characteristics and parameters of pristine single-walled carbon nanotube (SWCNT) films suspended over the hole. This allowed us to design a bolometer with a unique speed of response parameters owing to the low heat capacity of the sensor (film thickness ~40 nm) and to increase its sensitivity due to the low thermal conductivity between the sensor and substrate. Herewith, as is shown below, nanotubes have a low absorption coefficient in the wavelength range of 3–10 μm. To increase the bolometer sensitivity in this range, we have also studied various hybrid materials representing a SWCNT film coated with graphene. It is known that graphene is a unique absorber, because a monoatomic graphene layer with a thickness of only 0.35 nm absorbs 2.3% of radiation in a wide wavelength range [22]. This means that the application of several tens of graphene layers allows one to increase substantially the absorption coefficient, while the effect of graphene on the thermal capacity and sensor response time are minimal compared to other types of black.

2. Measurement techniques

The schematic and photograph of the samples are given in Fig. 1. 0.2-μm-thick gold contacts on a titanium and platinum sublayer were preliminary thermally deposited onto a circular quartz substrate with a diameter of 17 mm and thickness of 4 mm on both sides of the hole with a diameter of 6 mm located in the middle of the substrate. The selection of these materials is stipulated by several reasons. Firstly, quartz has a comparatively low thermal conductivity (1.38 W m^{-1} K^{-1}) which increases the sensor sensitivity. Secondly, gold is virtually not oxidised compared, for example, with copper, and the work function of gold is 4.8 eV which is close to the work function of nanotubes (4.5–5.0 eV). In addition, the deposition of a

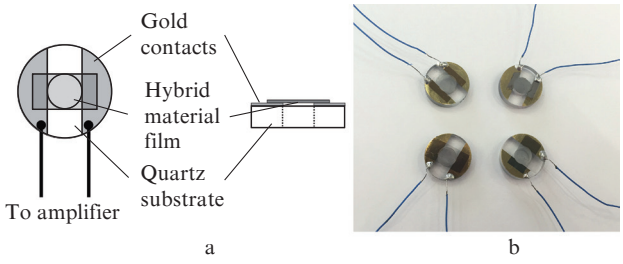

Figure 1. (a) Schematic and (b) photograph of bolometric sensor samples.

film of nanotubes onto wide flat contacts can significantly reduce the noise level at the contacts.

The SWCNT films were used as the sensor material. Carbon nanotubes were synthesised by chemical vapour deposition from the gas phase, carried out by thermal decomposition of ferrocene vapour [$Fe(C_5H_5)_2$] in the atmosphere of carbon monoxide (CO). The SWCNTs were collected on a cellulose filter placed at the reactor outlet [23, 24]. The thickness of the films with randomly oriented SWNTs formed on the filter surface is determined by the collection time; in our case, it was about 40 nm, the transparency of the film at a wavelength of 550 nm being equal to 80%. The obtained film was transferred directly from the filter onto the substrate in such a way that a considerable part of the film covered the contacts (dry transfer process from the filter is quite simple and described in detail, for example, in [25]). This method allows one to obtain relatively fast a very durable and thin free-standing film with a rather large area of randomly distributed pristine carbon nanotubes interlinked by the van der Waals forces.

Using different methods, graphene was deposited atop three samples out of four (see Table 1). For sample No. 2, a film of graphene was deposited from a solution of reduced graphene oxide in ethylene glycol (Akkolab, Moscow). Before this, ethanol had been dripped from above into a pre-heated solution to form a dense graphene film on the ethylene glycol surface. SEM studies showed that the film obtained by this method consists of layers of interlinked large graphene flakes with small gaps. These layers have a nonuniform thickness of tens to hundreds of nanometers. Graphene, having been previously transferred from a solution in ethylene glycol onto a quartz substrate, was applied onto sample No. 3 using the dry transfer technique. For comparison of samples, Table 1 shows an approximate number of graphene layers produced in various ways. It was calculated by the fraction of absorbed radiation at a wavelength of 550 nm on the assumption that each layer absorbs 2.3%. This is only an estimation value because graphene in our case does not lie uniformly but forms separate flakes, with a number of layers that can greatly exceed the average estimation over the sample. An aqueous dispersion of graphene oxide (Akkolab) was applied in three passes onto sample No. 4, preheated to 200 °C, from a distance of 100 mm by means of an aerodynamic spray. After that, graphene oxide has been recovered for 4 min by heating the sample to 300 °C [26]. This made it possible to obtain hybrid SWCNT + graphene samples with varying amounts of graphene and hence different absorption coefficients. IR transmission spectra of all the samples are shown in Fig. 2.

The following parameters were selected to determine the efficiency of the bolometer sensor samples: spectral characteristic (dependence of the bolometer sensitivity on the incident

Table 1. Samples of bolometric sensors with different absorbers.

Sample number	Sensor material, transmittance at λ = 550 nm	Absorber material, number of layers	Method of absorber deposition	Transmittance of the sample with an absorber at λ = 5 μm
1	SWCNT, 80%	No	–	95%
2	SWCNT, 80%	Graphene, ~40 layers	Transfer from a solution in ethylene glycol	17%
3	SWCNT, 80%	Graphene, ~10 layers	Dry transfer from a quartz substrate	68%
4	SWCNT, 80%	Graphene oxide, reduced by heat	Aerodynamic spraying	95%

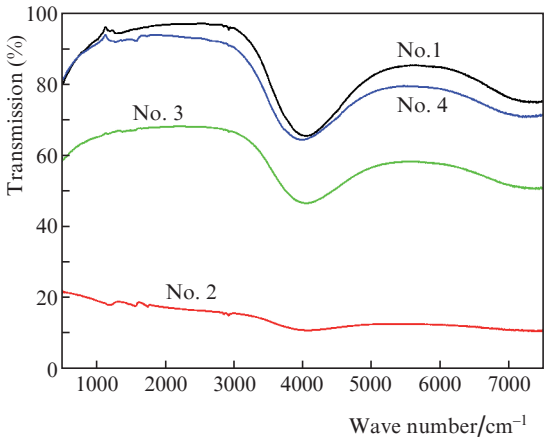

Figure 2. IR transmission spectra of bolometric sensors: sample No. 1 (pristine SWCNTs), sample No. 2 (SWCNT + 40 graphene layers), sample No. 3 (SWCNT + 10 graphene layers) and sample No. 4 (SWCNT + reduced graphene oxide).

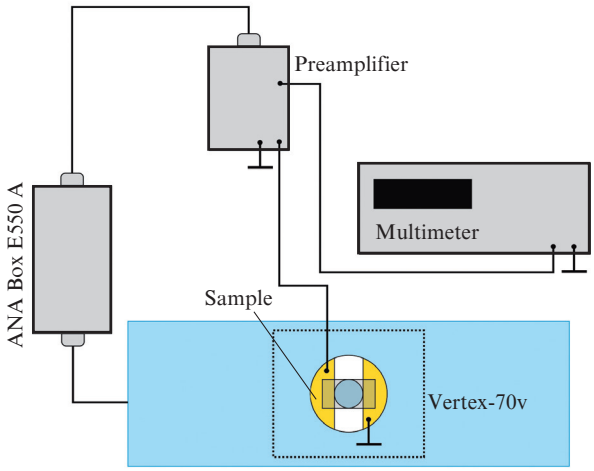

Figure 3. Scheme of measurement of the spectral characteristics of the bolometer.

radiation wavelength), voltage sensitivity (ratio of the bolometer voltage response to the incident radiation power), time constant, or response time (characterises the detector operating speed) and noise equivalent power (NEP).

To measure the bolometer's spectral characteristics in the range of 370–8000 cm^{-1} (1.25–27 μm), a standard globar forming part of a Vertex-70v FTIR spectrophotometer (Bruker, Germany), the spectrum of which is close to the blackbody spectrum, was used as a source of IR radiation. The modulated radiation of the globar was fed to the sample under study. To enhance the bolometer sensitivity, an aluminium mirror was mounted directly behind the sample, which allowed us to increase the amount of the absorbed radiation energy in the transparent samples. By means of thin wires, the sample contacts were soldered to the input of a special low-noise two-cascade preamplifier, the first-cascade gain of which could be varied depending on the load resistance: $K_{amp} = R_{fb}/R_{bol}$, where R_{fb} is the feedback resistance, which equals either 10 or 100 kΩ depending on the switch position, and R_{bol} is the resistance of the bolometric sample. A preamplifier was connected to the spectrophotometer input through the ANA Box E550 A (Bruker) console, which served as an analogue-to-digital converter and also as an additional preamplifier. The voltage of ±12 V was fed to the preamplifier via the console from a special low-noise source being part of the measuring circuit of the spectrophotometer. The scheme of the measurements is shown in Fig. 3.

Thus, in this scheme, the bolometric sample acts as a spectrophotometer detector. The spectral response of the sample to the modulated IR radiation of the globar is measured. In this case, each wavelength corresponds to a specific signal modulation frequency. To exclude spectral characteristics of the globar, the bolometer spectral response is normalised to the globar spectrum measured using a standard pyroelectric sensor of the spectrophotometer. In the investigated frequency range, spectral characteristic of a standard sensor is taken virtually constant. By means of this approach, the bolometer's spectral characteristic in relative units is determined. All spectral characteristics are also normalised by the gain of the first-cascade preamplifier since it depends on the sample resistance.

In measuring the voltage sensitivity R_v, the time constant τ and the noise equivalent power P_n, a laser module with an output power of 12.5 mW, a wavelength of 650 ± 5 nm and a beam diameter of no more than 5 mm was used as a source of optical radiation. Laser radiation was modulated by rectangular pulses, the frequency and duration of which were varied within a wide range depending on the sample performance. A laser beam was passed through the spectrophotometer's front window into the Vertex-70v sample compartment. To measure R_v and τ, a voltage signal from the first-cascade preamplifier was fed to an oscilloscope. The voltage sensitivity of the bolometric sample was calculated by the formula:

$$R_v = \frac{\Delta U}{P_{las} K_{amp}}, \quad (3)$$

where ΔU is the rectangular pulse response amplitude measured on the oscilloscope; P_{las} is the laser radiation power;

and K_{amp} is the first-cascade amplifier gain. Thus, the absolute voltage response of the bolometer to monochromatic radiation at a wavelength of 650 nm is determined. The time constant of the sample is determined by the trailing edge of the response pulse (by the 1/e signal level of the maximal amplitude).

The same scheme was used to measure the noise equivalent power P_n; however, the signal from the preamplifier was fed not to the oscilloscope but to the input of electronic recording system circuit of the Vertex-70v spectrophotometer. Thus, the noise and signal levels in a specified frequency band were measured ($\Delta f = 1$ Hz). It was assumed that the levels of noises introduced additionally on all cascades of preamplifiers are much lower than the noise level of the bolometer itself. The modulation frequency of laser pulses for each sample was deteremined to optimise the signal-to-noise ratio in the selected frequency band. The equivalent noise power is determined by the formula:

$$P_n = \frac{P_{las}}{\mathrm{SNR}\sqrt{\Delta f}}, \quad (4)$$

where SNR is the signal-to-noise ratio.

To determine the optimum ambient parameters which ensure the most effective bolometer operation, the dependences of the bolometer parameters on the ambient temperature and pressure were measured for some of the samples. With this aim in view, the bolometric sensor was preliminary placed into a special vacuum cell (VT cell GS21525) connected to a HICube 80 ECO pump by means of a Pfeiffer MPT 100 pressure gauge and a SPECAC 6100+ temperature controller. The cell placed inside the spectrophotometer is designed in such a way that the contacts from the sample can be brought outside and connected to the preamplifier input. Cooling to temperatures of –175 °C was carried out with liquid nitrogen. By using a pressure sensor and a pump, the required pressure of 2×10^{-7} – 1 bar was set inside the cell.

3. Experimental results and discussion

Figure 4 shows the spectral sensitivity of the samples listed in Table 1, measured at a pressure of 1 mbar (inside an evacuated measuring chamber of the spectrophotometer) and room temperature. If we compare the transmission spectra of the samples (see Fig. 2) with their spectral bolometric sensitivities, it is clearly seen that the spectral responses are modulated by the absorption coefficients of the samples. For example, a dip in the spectral characteristics at the wavelengths from 3 to 10 μm (1000–3000 cm^{-1}), which corresponds to high transmission of IR radiation by nanotubes, is clearly observed for the sample No. 1 (pure SWCNT). In contrast, the sensitivity peak is located at the wavelength of 2.5 μm (4000 cm^{-1}) which corresponds to the peak of the absorption coefficient. Hybrid sample No. 4 (SWCNT + reduced graphene oxide) is more sensitive in this range due to the increased absorption.

It can be seen that the well-absorbing samples (Nos 2 and 3) have a more uniform spectral sensitivity in this wavelength range of IR radiation (from 1.25 to 27 μm). On the other hand, the spectral response amplitude of the samples with a thick absorber is lower than that of the sample tubes without an absorber, or with a thin absorbing layer, especially at low wavelengths. This is due to the fact that, as shown below, 'thick' samples have a much lower response time. Since the radiation of each wavelength of the FTIR spectrophotometer

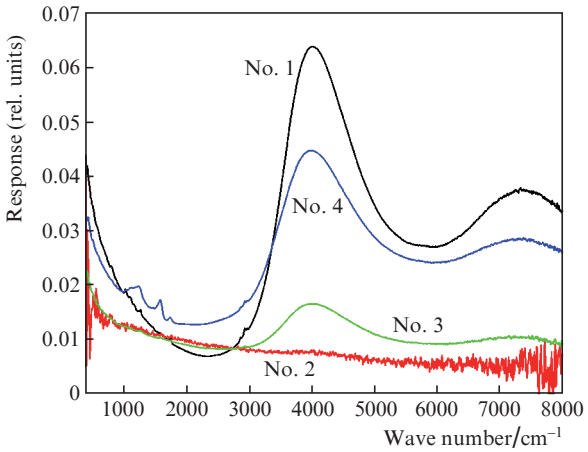

Figure 4. Spectral characteristics of samples of pure SWCNTs and hybrids with different absorbers at room temperature and a pressure of 1 mbar: sample No. 1 (pure SWCNTs), sample No. 2 (SWCNT + 40 graphene layers), sample No. 3 (SWCNT + 10 graphene layers) and sample No. 4 (SWCNT + reduced graphene oxide).

is modulated at a certain frequency (the shorter the wavelength, the greater the frequency), slow bolometers just 'do not feel' high modulation frequencies of radiation. This fact must be taken into account when comparing the samples.

More precise conclusions on the bolometer efficiency can be derived in accordance with the absolute voltage sensitivity, time constant and NEP given in Table 2. These measurements were carried out at room temperature and a pressure of 1 mbar. The waveform response to the modulated radiation represents a train of rectangular pulses. To illustrate the sample response speed to switching on/off laser radiation, Fig. 5 presents the trailing edges of the voltage responses for bolometric samples. For clarity, all responses are normalised to the amplitude maximum. It can be seen that sample No. 1 (pristine SWCNTs) has the highest response time. Its time constant at a pressure of 1 mbar and room temperature constitutes 2.6 ms. The time constant of sample No. 4 (a hybrid of SWCNTs and reduced graphene oxide) is slightly greater: it amounts to 3.3 ms. The voltage sensitivity of these two samples is approximately the same and amounts to ~1.5 V W^{-1}. The response time of sample Nos 2 and 3 is 37 and 14 ms, respectively. This is due to the fact that the absorber layer contributes to the heat capacity of the sensor, which has a negative impact on the performance [see (2)]. Thus, the hybrid sample with the thickest graphene layer (~40 layers), due to high absorption, turned out to be the most sensitive to pulsed laser radiation (2.4 V W^{-1}). The total heat capacity of the tubes and coatings can be inferred by the sample response time, while the efficiency of absorption and heat transfer from the absorber to the tubes determines the voltage sensitivity. In

Table 2. Values of bolometric parameters for the samples with different absorbers, measured at room temperature and a pressure of 1 mbar.

Sample number (absorber)	R_v/V W^{-1}	τ/ms	P_n/ 10^{-9} W $Hz^{-1/2}$
1 (without absorber)	1.58 ± 0.15	2.6 ± 0.3	8.8 ± 2.0
2 (graphene, ~40 layers)	2.4 ± 0.3	37 ± 3	19 ± 5
3 (graphene, ~10 layers)	1.38 ± 0.10	14 ± 1	9 ± 3
4 (reduced grapheme oxide)	1.52 ± 0.10	3.3 ± 0.3	2.0± 0.4

general case, the addition of an absorbing layer enhances the sample sensitivity, but strongly affects the operating speed. As for the NEP, the best characteristics are exhibited by hybrid sample No. 4 and pristine SWCNT sample No. 1. Generally, we can assert that the presence of an absorber apparently adds thermal and current noises to the bolometer's voltage response.

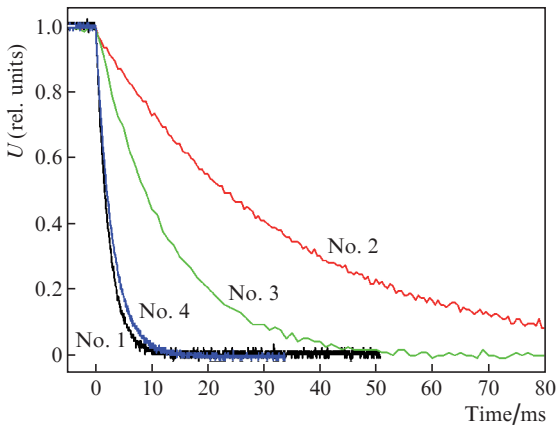

Figure 5. Normalised voltage responses of the samples with different absorbers for pulsed laser irradiation at room temperature and a pressure of 1 mbar: sample No. 1 (pristine SWCNTs), sample No. 2 (SWCNT + 40 graphene layers), sample No. 3 (SWCNT + 10 graphene layers) and sample No. 4 (SWCNT + reduced graphene oxide).

Figure 6 shows the voltage sensitivity and time constant as functions of pressure in the cell in the range of $2 \times 10^{-7} - 1$ bar. The character of the dependences for both samples is similar. In lowering the pressure in the cell, initially the sensitivity remains virtually unchanged up to 10 mbar. The further lowering of the pressure results in a sharp increase (by 2–3 times) in sensitivity. This is due to the fact that when the sell is evacuated, heat conduction and convection through the air cease to contribute to heat transfer. The sample is only cooled by radiation and through the contact with the substrate, the cross-sectional area of which is small. Thus, ceteris paribus, heating of the sample by radiation in vacuum is stronger, and its sensitivity increases.

It is obvious that, as the pressure decreases, the time constant, which is inversely proportional to the thermal conductivity, also increases. This is actually observed at pressures below 1–10 mbar: the time constant under high vacuum increases by 1.5–2 times. On the other hand, the sample response time sharply increased at pressures above 100 mbar. Apparently, this reflects a contribution of the layer of air to the thermal capacity of the system. The irradiated sample heats the adjacent layer of air, thermal conductivity of which is low. As a result, the sample reacts slowly to the changes in irradiation.

Thus, with regard to the response time, the pressure range 10^{-3}–10^{-1} bar is optimal for a bolometer of this type, despite the fact that the sensitivity is better at lower pressures. In addition, high vacuum is technologically more difficult to maintain.

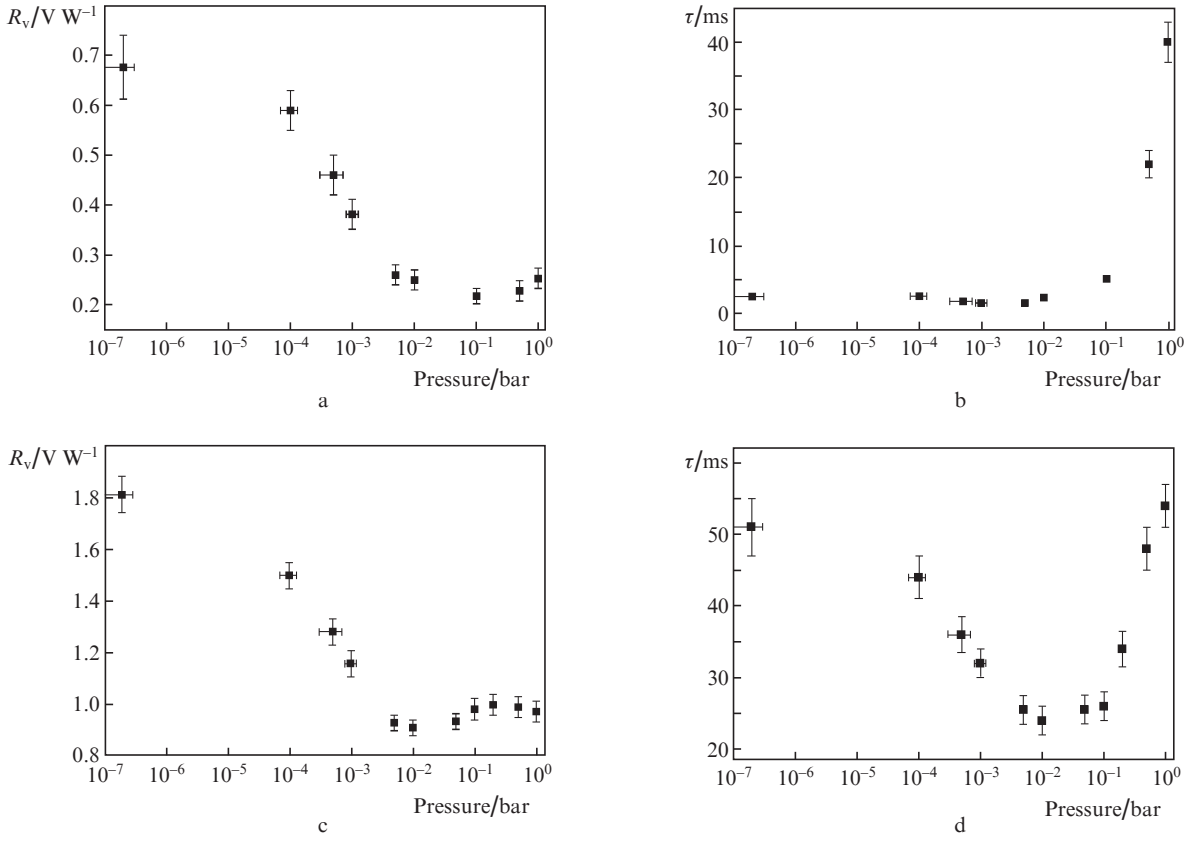

Figure 6. Voltage sensitivity and time constant as functions of ambient pressure for (a, b) sample No. 1 (pristine SWCNT) and (c, d) sample No. 2 (SWCNT + 40 graphene layers) at room temperature.

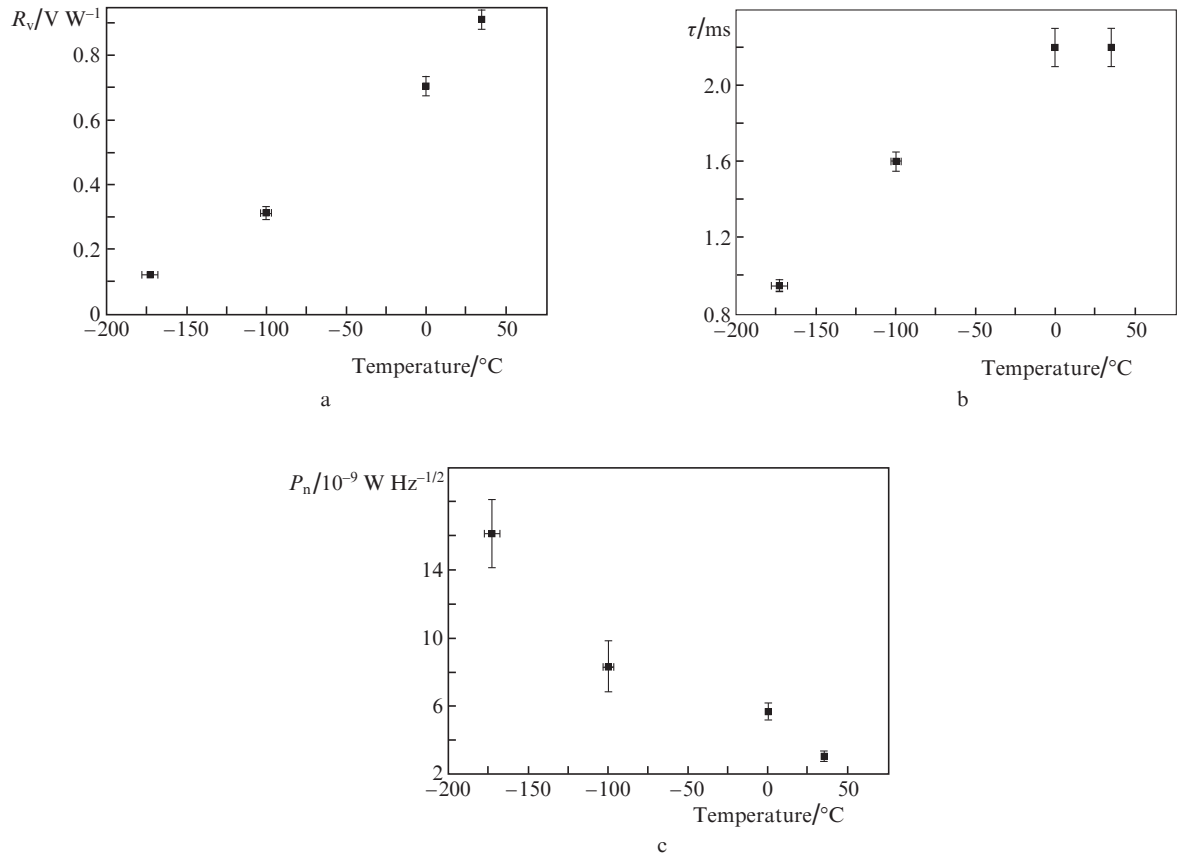

Figure 7. (a) Voltage sensitivity, (b) time constant and (c) NEP as functions of temperature for sample No. 4 (SWCNT + reduced graphene oxide) at a pressure of 1 mbar.

The voltage sensitivity, time constant and NEP as functions of temperature are shown in Fig. 7 for sample No. 4. The temperature drops significantly with lowering the sample sensitivity. This may be stipulated by several reasons. Firstly, with decreasing temperature, the temperature coefficient of the sample resistance also decreases. Secondly, due to the fact that the SWCNTs we have used have metallic nature of the resistance dependence on temperature, the sample resistance decreases several times down to liquid nitrogen temperature. It is also possible that thermal conductivity of the sample grows with cooling. The latter assumption is confirmed by the temperature dependence of the time constant shown in Fig. 7b. A decrease in temperature from +33 °C to –173 °C increases twice the sample response time. The noise equivalent power increases with decreasing temperature, which is associated with a reduction in the sample sensitivity. Thus, the NEP increases only fivefold, whereas the signal level falls nine times. Obviously, this is because the total noise level and the temperature-related resistance also decrease with decreasing temperature. From this we may conclude that the additional cooling of the bolometer based on the nanotubes we have used in this work is inadvisable due to a strong reduction in sensitivity while cooling. The sensors made of nanotubes with semiconductor properties can have different nature of the temperature sensitivity dependence due to an increase in the α coefficient at liquid nitrogen temperatures.

4. Conclusions

A bolometric sensor was constructed based on suspended carbon nanotubes obtained by aerosol synthesis, possessing a small response time of 2.6 ms at room temperature and 1 mbar pressure, which is several times better than the response time of commercial bolometers [27]. By lowering the temperature to –175 °C, the bolometer response time may be reduced to 1 ms.

The application of an additional layer of graphene onto the film of nanotubes allows increasing the bolometer voltage sensitivity by 1.5 times due to increased absorption in comparison with a sample of pristine nanotubes. This considerably reduces the bolometer response time, since the addition of the absorbing material increases the thermal capacity of the sensor.

All the bolometer samples are sensitive to IR radiation in the range of 1.3–27 μm at room temperature. It is shown that additional cooling of the bolometer to –175 °C offers no advantage in the sensitivity and noise characteristics, although in this case the response time is decreased. The sensitivity increases by reducing the ambient pressure to 2×10^{-7} bar, while the optimal value of the response time is observed at a pressure of 10^{-3}–10^{-1} bar.

The studies we have conducted allow us to offer the carbon nanotubes, obtained by aerosol synthesis, as a promising sensor material for the production of ultra-fast bolometers

and micro-bolometer arrays. In the future, we plan to improve the sensitivity and response time of the bolometric sensor at the expense of selecting the tubes with a high temperature resistance coefficient, using an optimal substrate configuration, and also optimising the preamplifier parameters and the bolometer connection circuit.

Acknowledgements. The authors are grateful to A. Gorkina and E. Gilshteyn for their assistance in the preparation of samples and measurements.

The work was supported by the Ministry of Education of the Russian Federation (Project No. RFMEFI58114X0006).

References

1. Filachev A.M., Taubkin I.I., Trishenkov M.A. *Tverdotel'naya elektronika. Fotoresistory i photodetectory* (Solid-State Electronics. Photoresistors and Photodetectors) (Moscow: Fizmatkniga, 2012).
2. Rogalski A. *Infrared Detectors* (Boca Raton, Florida, USA: CRC Press, Taylor & Francis Group, 2011).
3. Rogalski A. *Opto-Electron. Rev*., **20** (3), 279 (2012).
4. Smuk S., Kochanov Yu., Petroshenko M., Solomitskii D. *Komponenty i tekhnologii*, **1**, 152 (2014).
5. Ado J., Dresselhaus G., Dresselhaus M.S. *Carbon Nanotubes. Advanced Topics in the Synthesis, Structure, Properties and Appliations* (Berlin, Helderberg: Springer-Verlag, 2008).
6. Freitag M., Martin Y., Misewich J.A., Martel R., Avouris Ph. *Nano Lett*., **3** (8), 1067 (2003).
7. Matsuoka Y., Fujiwara A., Ogawa N., Miyano K., et al. *Sci. Technol. Adv. Mater*., **4** (1), 47 (2003).
8. Matsuoka Y., Suematsu H., Ogawa N., Miyano K., et al. *Carbon*, **42** (5), 919 (2004).
9. Zhang J., Xi N., Chan H., Li G. *Proc. SPIE Int. Soc. Opt. Eng*., **6395**, 63950-A (2006).
10. Avouis P., Afzali A., Appenzeller J., Chen J., et al. *IEDM Tech. Digest*, 525 (2004).
11. Misewich J.A., Martel R., Avouris P., et al. *Science*, **300**, 783 (2003).
12. Jariwala D., Sangwan V.K., Lauhon L.J., Marks T.J., Hersam M.C. *Chem. Soc. Rev*., **42**, 2824 (2013).
13. Buchs G., Bagiante S., Steele G.A. *Nat. Commun*., **5**, 4987 (2014).
14. Itkis M.E., Borondics F., Yu A., Haddon R.C. *Science*, **312**, 413 (2006).
15. Haddon R.C., Itkis M.E. US Patent, US7723684 B1 (2010).
16. Cech J., Swaminathan V., Wijewarnasuriya P., Currano L.J., Kovalskiy A., Jain H. *Proc. SPIE Int. Soc. Opt. Eng*., **7679**, 76792N (2010).
17. Lu R., Li Z., Xu G., Wu J.Z. *Appl. Phys. Lett*., **94**, 163110 (2009).
18. Pradhan B., Setyowati K., Liu H., Waldeck D.H., Chen J. *Nano Lett*., **8** (4), 1142 (2008).
19. Aliev A.E. *Infr. Phys. Technol*., **51**, 541 (2008).
20. Glamazda A.Y., Karachevtse V.A., Euler W.B., Levitsky I.A. *Adv. Funct. Mater*., **22**, 2177 (2012).
21. Vera-Reveles G., Simmons T., Bravo-Sanchez M., Vidal M.A., Navarro-Contreras H., Gonzalez F. *ACS Appl. Mater. Interf*., **3**, 3200 (2011).
22. Katsnelson M.I. *Graphene: Carbon in Two Dimensions* (NY: Cambridge University Press, 2012).
23. Moisala A., Nasibulin A.G., Brown D.P., Jiang H., Khriachtchev L., Kauppinen E.I. *Chem. Eng. Sci*., **61**, 4393 (2006).
24. Tian Y., Zavodchikova M., Kivistö S., Nasibulin A.G., Zhu Z., Jiang H., Okhotnikov O.G., Kauppinen E.I. *Nano Research*, **4** (8), 807 (2011).
25. Nasibulin A.G., Kaskela A.O., Mustonen K., Anisimov A.S., et al. *ACS Nano*, **5**, 3214 (2011).
26. Gorkina A.L., Tsapenko A.P., Gilshteyn E.P., Koltsova T.S., Larionova T.V., Talyzin A., Anisimov A.S., Anoshkin I.V., Kauppinen E.I., Tolochko O.V., Nasibulin A.G. *Carbon*, **100**, 501 (2016).
27. Wood R.A. *Uncooled Microbolometer Infrared Sensor Arrays in Infrared Detectors and Emitters: Materials and Devices* (Boston, USA: Kluwer Acad. Publ., 2000).